J Fluoresc (2009) 19:733–740
DOI 10.1007/s10895-009-0469-8

ORIGINAL PAPER

Preparation and Non-Invasive In-Vivo Imaging of Anti-Adhesion Barriers with Fluorescent Polymeric Marks

Shih-Rong Hsieh · Chi-Jung Chang · Tzong-Der Way · Po-Cheung Kwan · Tsung-Wei Hung

Received: 31 October 2008 / Accepted: 30 January 2009 / Published online: 12 February 2009

Abstract Comb-like PEMLn polymers with pendent PEG-PLLA side chains were synthesized as tissue anti-adhesion barriers. The comb-like structure improved the flexibility of the films. Fluorescent polymer-biocompatible polymer guest-host materials were printed on the films as marking dots. Without sacrificing rats on different days after surgery, degradation behaviors of the marked films can be investigated non-invasively in the in-vivo imaging system (IVIS) by monitoring the location of fluorescent signals. Degradation properties of PEML1/G26L35 films were adjusted by incorporating G26L35 oligomers. PEML1 and PEML1/G26L35 films were very effective in preventing post-surgical tissue-adhesions. Degradation behaviors of various films observed in the animal study were consistent with those investigated by the in-vivo imaging method. Fluorescent polymer/biocompatible polymer blends were promising candidates for in-vivo imaging applications.

Keywords In-Vivo imaging · Non-invasive · Anti-adhesion · Fluorescent polymer · Fluorescence

C.-J. Chang (✉) · T.-W. Hung
Department of Chemical Engineering, Feng Chia University,
100, Wenhwa Road, Seatwen,
Taichung 40724, Taiwan
e-mail: changcj@fcu.edu.tw

S.-R. Hsieh
Department of Surgery, Taichung Veterans General Hospital,
Taichung 40724, Taiwan

P.-C. Kwan
Department of Pathology, Taichung Veterans General Hospital,
Taichung 40724, Taiwan

T.-D. Way
School of Biological Science and Technology,
College of Life Science, China Medical University,
Taichung 40724, Taiwan

Introduction

Undesirable tissue-adhesions after surgical treatment often induce severe problems such as chronic pelvic pain, bowel obstructions, and difficult reoperative surgery. Methods for reducing adhesion formation focused on applying barriers at the surgical surfaces and local delivery of anti-inflammatory or anti-fibrinolytic agents [1]. Polymeric films [2–5] and anti-inflammatory drug-loaded materials [6, 7] have been employed as barrier films or injectable barrier gel [8–10] to reduce postsurgical adhesion. Polylactide (PLLA) is one of the most widely used biomedical polymers because of its biodegradability and biocompatibility. However, its application has been limited because of its stiffness and hydrophobicity. Introducing polyethylene glycol (PEG) can enhance not only the flexibility and hydrophilicity [11–13], but also the anti-tissue adhesion [14] properties of PLLA films. PLLA-PEG block copolymers have been synthesized for drug delivery and tissue engineering applications [15–16].

Optical imaging using visible light is hindered by native biological fluorescence as well as light absorption and scattering by biological tissue constituents, such as amino acids, blood hemoglobin, and water. However, near-IR-emitting fluorescence imaging overcomes these limitations. Biological autofluorescence and absorbance are kept at their minima in the wavelength range of 600–900 nm. This region of the spectrum is suitable for in-vivo fluorescent imaging. [17–19]

The goal of this study is to develop new comb-like polymeric films as anti-adhesion barriers and a non-invasive method to investigate the degradation behaviors of the film by monitoring the location of the fluorescent signals. The effects of the polymer chemical structure (comb-like or linear) on the tissue anti-adhesion properties were evaluated. Marking dot array was made by dispensing

fluorescent polymer-biocompatible monomer guest-host materials on the tissue anti-adhesion films. Then, the printed dot-array was fixed by UV-curing of the monomer. As shown in Fig. 1, the marked anti-adhesion films were applied on the defects. The film started degrading. There were small fragments of the films migrated in the peritoneal cavities. When the film started degrading, there will be small fragments of the films migrated in the peritoneal cavities. In vivo degradation behavior can be assessed by measuring the photoluminescent signal distribution in the rats using a highly sensitive IVIS Imaging System.

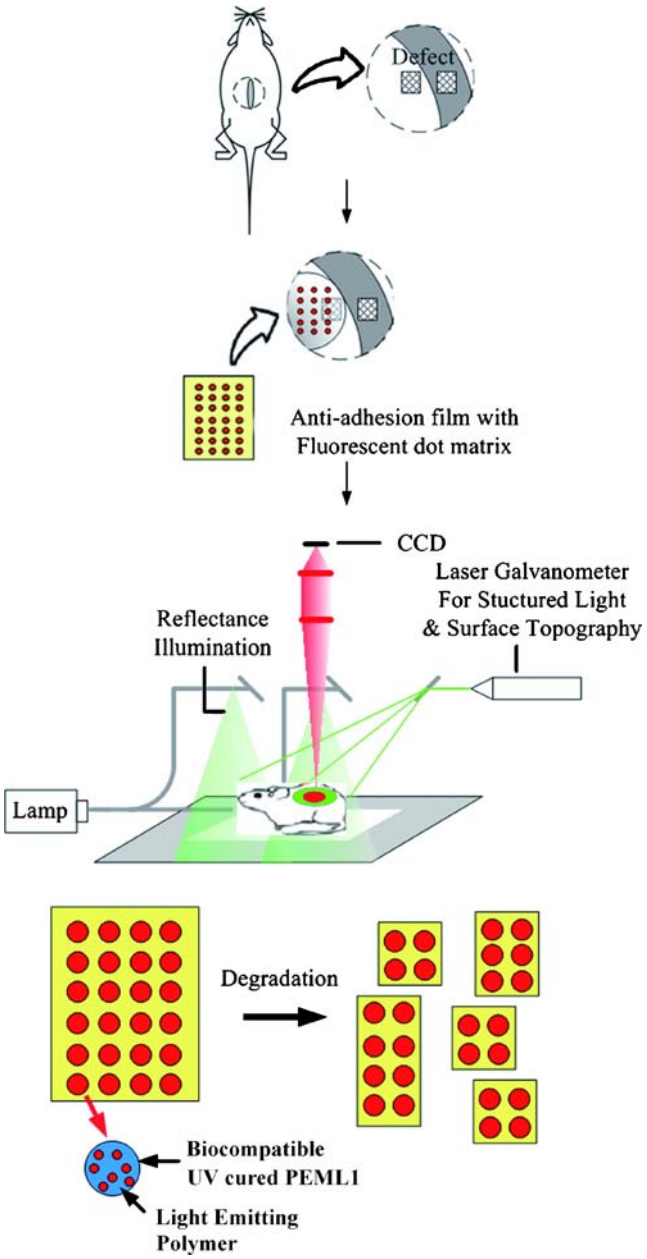

Fig. 1 Schematic illustration of implanting barrier films with fluorescent marks in rats and non-invasive observation of film degradation by in-vivo imaging system

Materials and methods

Lactide, polyoxyethylene glycerol, polyethylene glycol and poly(ethylene glycol) methacrylate (EM, average M_n ~526) were purchased from Aldrich co. Tin(II) 2-ethylhexanoate was supplied by Sigma co.

Preparation of films

Chemical structures of PEMLn polymer, G26Lm and P4KLx polymer were shown in Fig. 2. The symbols x, m and n represented the numbers of the lactide repeating units on the polymer. For example, the pendent PLLA-PEG side chains of PEML1 and PEML5 contained one and five lactide repeating units respectively.

The EMLn monomer was synthesized by a ring opening polymerization of L-lactide with poly(ethylene glycol) methacrylate (EM, average M_n ~526). Tin(II) 2-ethylhexanoate was used as a catalyst. Before the polymerization, lactide and EM were vacuum-dried at 40°C for 12 h. Lactide, EM and tin(II) 2-ethylhexanoate were heated to 100°C with continuous dry nitrogen purging. After 6 h, the monomer was cooled to room temperature, dissolved in dichloromethane, filtered, and precipitated in heptane. The EMLn monomer was dried under vacuum at 50°C for 24 h. G26Lm was synthesized by a similar procedure except replacing EM with polyoxyethylene glycerol (G26, oxyethylene repeating unit: 26) and changing the amount of lactide. Linear polymer P4KL60 were synthesized by a similar procedure except replacing G26 with polyethylene glycol (Mn=4000) and changing the amount of lactide. Poly[2-methoxy-5-(2-ethyl-hexyloxy)-1,4-phenylene vinylene] (MEH-PPV) was synthesized via the method which can be found elsewhere [20].

P4KL60 films were prepared by solvent casting. The EMLn monomers were mixed with 2-hydroxy-2-methyl-1-phenyl-propan-1-one (initiator) (weight ratio: monomer/initiator = 100/3). The solution was cast in the Teflon mold. The mixture was UV cured to prepare the comb-like PEMLn (n=y/2 as shown in Fig. 2a) film. PEML1/G26L35 film was made by a process similar to PEMLn film except G26L35 oligomer (weight ratio: PEML1:G26L35= 1:1) was incorporated. Red fluorescent polymer MEH-PPV, biocompatible EML1 monomer and photoinitiator 1-hydroxy-2-methyl-1-propane-1-one were dissolved in THF. The solution was printed as dot matrix on the anti-adhesion film. After removing the solvent, the mixture was UV cured to prepare the marking dots. The diameter of the marking dot is 2 mm. The photoluminescent (PL) images of the

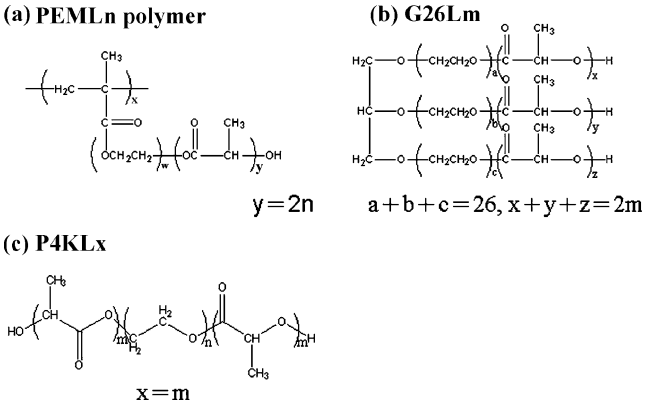

Fig. 2 Chemical structures of **a** PEMLn **b** G26Lm **c** P4KLx polymer

printed dots were observed by the fluorescence microscopy (Olympus).

Cytotoxicity test

MTT (3-(4,5-dimethylthiazol-2-yl)-2,5-diphenyl tetrazolium bromide) assay were used to determine the number of viable cell. Briefly, cells were seeded at a density of 1×10^4 cells into microtiter plate with 200 μl well culture medium overnight, then treated with various concentrations geraniin, and incubated for an additional 24 h. The effect of geraniin on cell growth was examined by the MTT assay. Briefly, 20 μl of MTT solution (5 mg/ml; Sigma Chemical) was added to each well and incubated for 4 h at 37°C. The supernatant was aspirated, and the MTT-formazan crystals formed by metabolically viable cells were dissolved in 200 μl of DMSO solvent. Finally, the absorbance was monitored by a microplate reader at a wavelength of 595 nm.

In vivo imaging

In vivo degradation behavior was assessed by measuring the photoluminescent property in the rat using a noninvasive imaging system (IVIS® Imaging System, Xenogen Corporation). As shown in Fig. 1, the rat was positioned on the object table inside the measurement cabin. It was exposed under a broad spot with even optical density. The emitted fluorescence from the rat was detected with the IVIS 200 cooled CCD camera system. Another laser was supplied as background light to get the surface topography. Living Image software (Xenogen Corp.) was used for data analysis as an overlay on IGOR software (Wavemetrics Corporation).

Preliminary animal study

The animal study was conducted under aseptic conditions. Rats were anesthetized with isoflurane (3.0%) and orally intubated, placed on a volume-cycled ventilator for continuous ventilation with room air supplemented with oxygen and isoflurane (1.5–3.0%). After anesthesia, the animals received surgical defects to their left peritoneal wall, intestine, surface of left lobe of liver. The animals underwent medium abdominal incision. The left lower abdominal wall was reflected. A 1×1 cm sized defect was created by removing the peritoneum and some associated muscle fibers. A similar size serosal defect was created on the intestine by rubbing an abrasive paper on the cecum surface just opposite to the defect of peritoneum. The left upper abdominal wall was reflected. A 1×1 cm sized defect was created by removing the peritoneum and some associated muscle fibers, and a similar size serosal defect was created on the surface of left lobe of liver by rubbing an abrasive paper on the liver surface just opposite to the defect of peritoneum. The anti-addition barrier films (3×3 cm in size) were then applied to and cover the serosal defects of small intestine, or liver. The control group did not receive implantation of artificial films. After 28 days, the peritoneum of the animal was examined by direct observation for adhesions under general anesthesia. Five animals were investigated for each kind of polymer sample.

Histological examination

The experimental rats were sacrificed on the 28th day after surgery to examine the adhesion formation at the injured site. The abdominal wall, intestinal wall and liver surface of the injured site were removed and fixed in 10% formalin solution. The tissues were processed by the standard procedure for histological examinations.

Results and discussions

Marking dots

In order to investigate the degradation behaviors of the anti-adhesion film by monitoring the location of the fluorescent signals, the dots should be fixed on the biodegradable film and biocompatible. The red fluorescent polymer was mixed with biocompatible UV-curable monomers. The mixtures were printed on the anti-adhesion films and UV cured as the marking dots. Figure 3 showed the photoluminescent (PL) images of the printed dots excited by light with different wavelength. The PL images were observed by the fluorescence microscopy. The UV cured biocompatible PEML1 dots exhibited blue PL light when they were excited by UV light (Fig. 3a1). However, no PL signal was observed when the dots were excited by blue or green light (Fig. 3a2, a3). The MEHPPV dots exhibited yellow PL

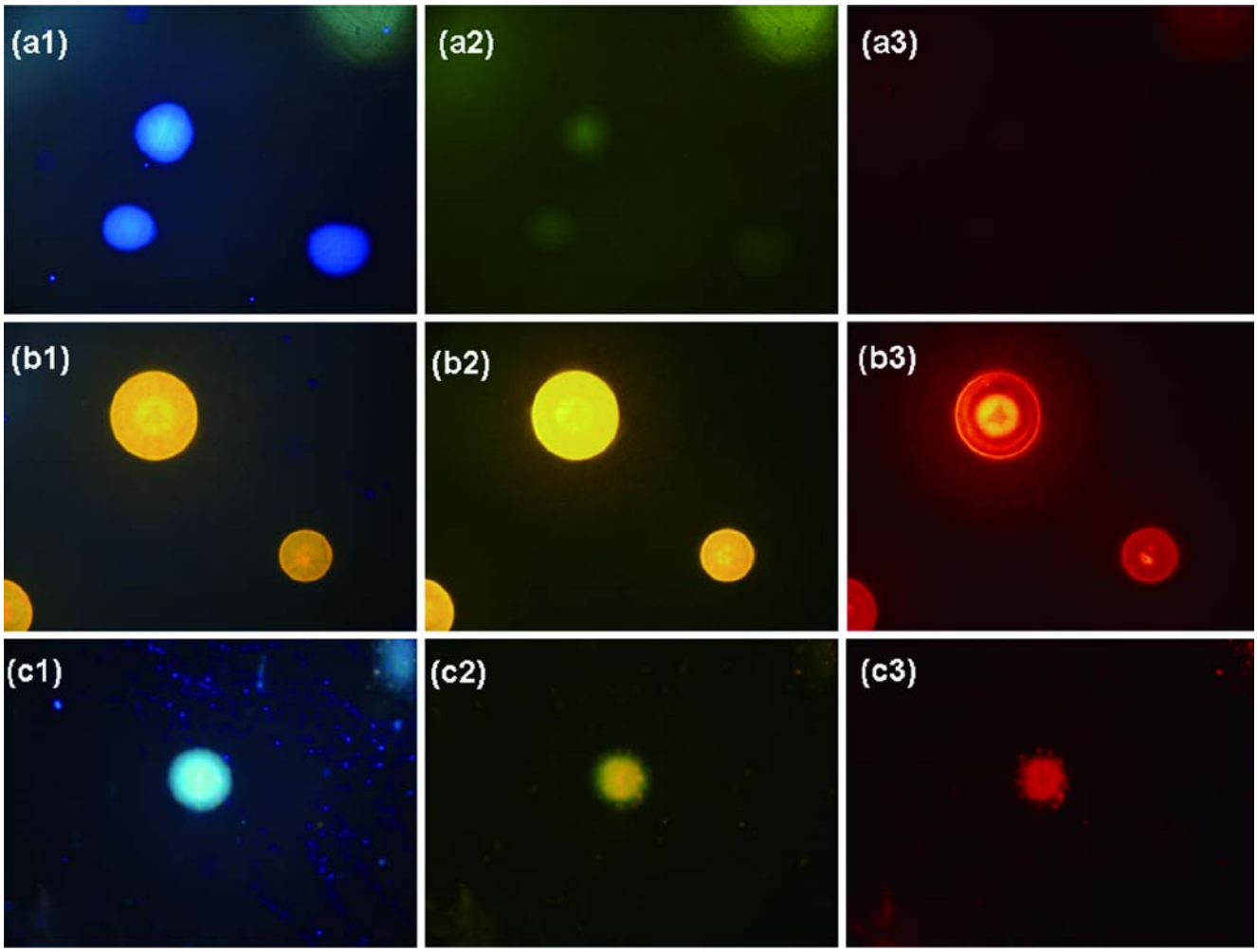

Fig. 3 Photoluminescent images of the printed **a** MEHPPV **b** PEML1 **c** MEHPPV/PEML1 dots excited by (1) UV (2) blue (3) green light

light when excited by UV or blue light (Fig. 3b1, b2). However, red PL signals were observed when the dots were excited by green light (Fig. 3b3). Figure 3 c showed the PL images of the MEHPPV/cured PEML1 dots. The dot exhibited blue PL light at the edge and yellowish blue PL light near the center when it was excited by UV light (Fig. 3c1). Yellow PL dot was observed when excited by the blue light (Fig. 3c2). The diameter of the PL dot was close to the yellowish blue central region shown in Fig. 3c1. Smaller red PL dot was observed when excited by the green light (Fig. 3c3). The diameter of the red PL dot was close to the yellowish blue central region shown in Fig. 3c1. Serrano et al. [21] reported the imaging of phase-separated polymer blends by fluorescence microscopy. Phase separation in two types of domains was observed by epifluorescence microscopy. In this study, MEHPPV and PEML1 showed different PL light when excited by UV light. The spatial distribution of fluorescent polymer (MEHPPV) and biocompatible polymer (PEML1) in the dots can be monitored by fluorescence microscopy. The results suggested that MEHPPV located near the center of the dot and PEML1 was distributed at the outer edge.

Figure 4 exhibited the contact angle of water droplet on the MEHPPV film and the MEHPPV/PEML1 film. MEHPPV is a hydrophobic polymer. The contact angle of MEHPPV film is 89° (Fig. 4a). However, the contact angle of the MEHPPV/PEML1 film became 14° (Fig. 4b). Cured PEML1 polymer is hydrophilic because of the polyethylene-oxide segment on the side chain. In addition to fix the dots on the anti-adhesion film, the cured PEML1 also helped to improve the hydrophilic properties of the printed MEHPPV/PEML1 dots. Figure 3 reveals that PEML1 located at the outer edge of the dot. Cured PEML1 polymers not only acted as binders to fix the marks on the film but also made the marks hydrophilic and biocompatible.

Cytotoxicity

Since the polymers are to be used for biomedical applications, the issue of cytotoxicity has to be addressed.

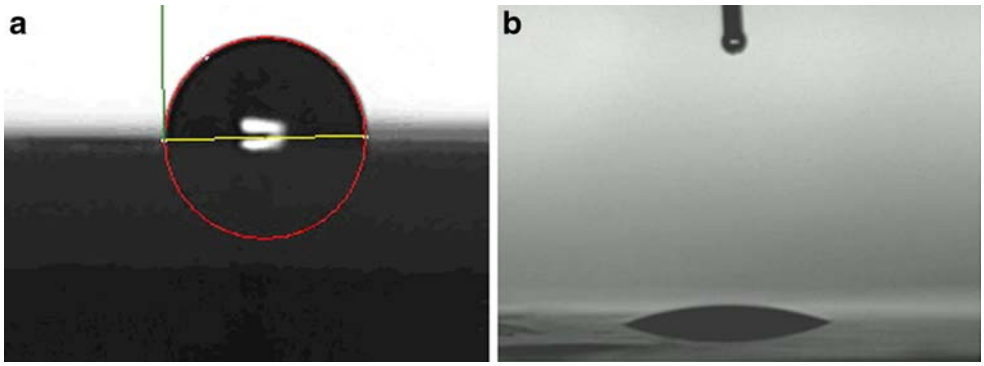

Fig. 4 Contact angle images of **a** MEHPPV film **b** MEHPPV/PEML1 blend film

The viability of the fibroblast NIH3T3 cells in the presence of PEML1, PEML5 and PEML1-G26LA35 were assessed relative to cells in the control experiment (no files present) using the MTT assay (see Experimental) which has been described as a very suitable method for the detection of biomaterial toxicity. The viability remains high (as compared to the nontoxic control) after 24 h of incubation, as shown in Fig. 5. This confirms the low toxicity of the synthesized polymers to fibroblast NIH3T3 cells.

Monitoring degradation behavior of films in vivo

In-vivo degradation properties are very important for the application of biodegradable materials. Wang et al. [22] measured the degradation of polygalacturonic acid (PGA) membranes in vivo by monitoring the decreasing molecular weight of Rhodamine-labeled PGA molecules. Rhodamine-PGA conjugated film was implanted in the rat's abdominal cavity. Rat peritoneal fluids were collected on different day after the operation, and the molecular weights of Rhodamine-labeled PGA molecules were determined by Gel Permeation Chromatography (GPC) with an RF detector (excitation at 545 nm and emission at 570 nm) [22]. Recently, optical imaging is more attractive in the diagnostic application because of its easy operation, better temporal resolution and relative low cost. In this study, the fluorescent signal distributions of the marked films in the rat 21 days after implantation were observed to monitor the degradation behavior non-invasively. Representative rats from each treatment groups are shown in Fig. 6. The color overlay on the image represents the photons emitted from the animal in accord with the pseudo-color scale shown next to the images. Red represents the highest photons/second, whereas blue represents the lowest photons/second. The fluorescent signal of marked PEML1 film located near the initial site implanted (Fig. 6a). It reveals the integrity of the film. The fluorescent signal of PEML5 film spread over a wider region (Fig. 6b). The film started degrading. There were small fragments of the films migrated in the peritoneal cavities. The fluorescent signal of P4KL60 film was weaker than those of PEML1 and PEML5 films (Fig. 6c). The degree of degradation of P4KL60 film was higher than the other two. Weak, small and widespread fluorescent signal was found in the PEML1/G26L35 film. It had been broken into small pieces (Fig. 6d).

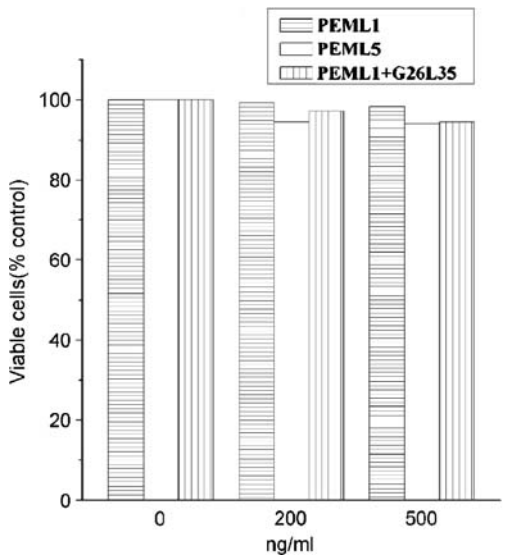

Fig. 5 Cytotoxicity of different concentrations of PEML1, PEML5 and PEML1/G26L35 films polymers on NIH3T3 cells

Animal implant study

Figure 7 shows the images of the injured sites in the operated rats with different treatment 28 days after surgery. The films were placed between intestines and peritoneal defects. Some films were covered between liver and peritoneal defects of rats. The anti-adhesion potentials of different films were evaluated. All the defects without incorporation of artificial films (control) showed dense adhesion with difficult dissection (Fig. 7a). The application of the P4KL60 film to the defects (Fig. 7b) showed less adhesion than the control group. Some adhesions formed between the intestine and the peritoneal wall. The P4KL60 film was a little stiff. Implanting stiff films in the body may mechanically stimulate the surrounding soft tissues and result

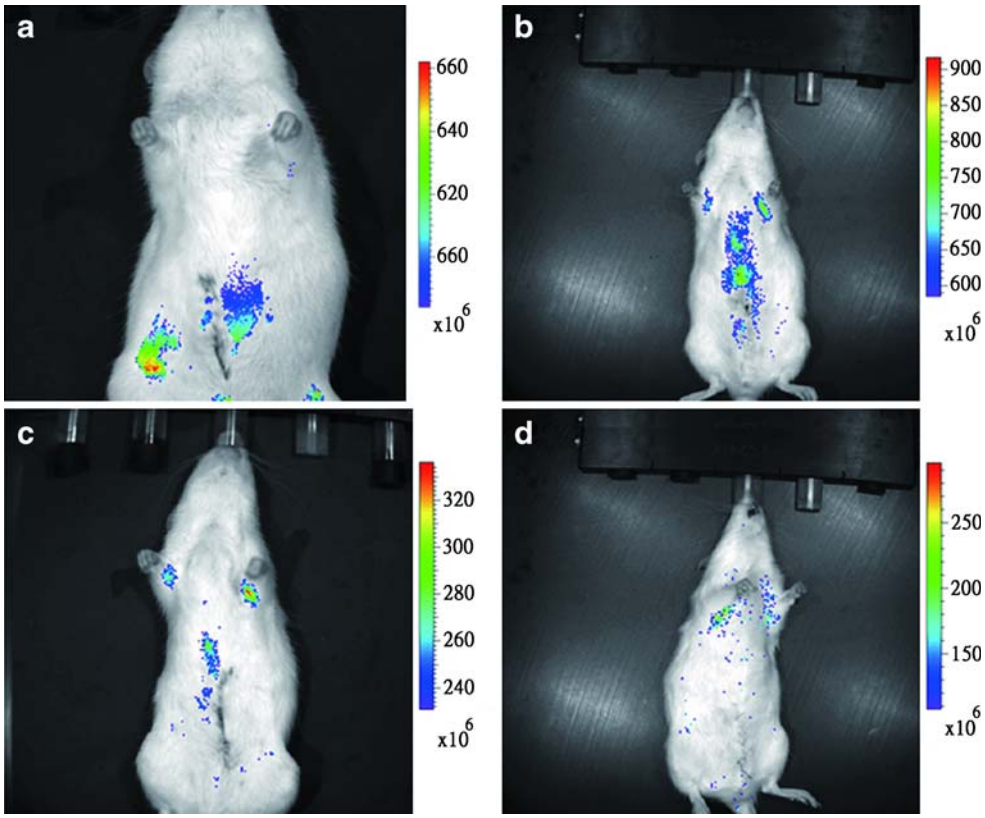

Fig. 6 In vivo observation of the film decomposition by monitoring the photoluminescent signal distribution in the rats 21 days after implanting the marked **a** PEML1 film **b** PEML5 film **c** P4KL60 film **d** PEML1/G26L35 film

in adhesion of the tissue. The formation of a comb-like structure with pendent PEG/PLLA side chains effectively improved the flexibility of the films. PEML1 and PEML5 films were flexible at room temperature. All the defects covered with the PEML1 and PEML1/G26L35 films presented no adhesion (Fig. 7c and d). Several fragments of the films left (Fig. 7c) and freely migrated in the peritoneal cavities. The fragments of the PEML1/G26L35 films were

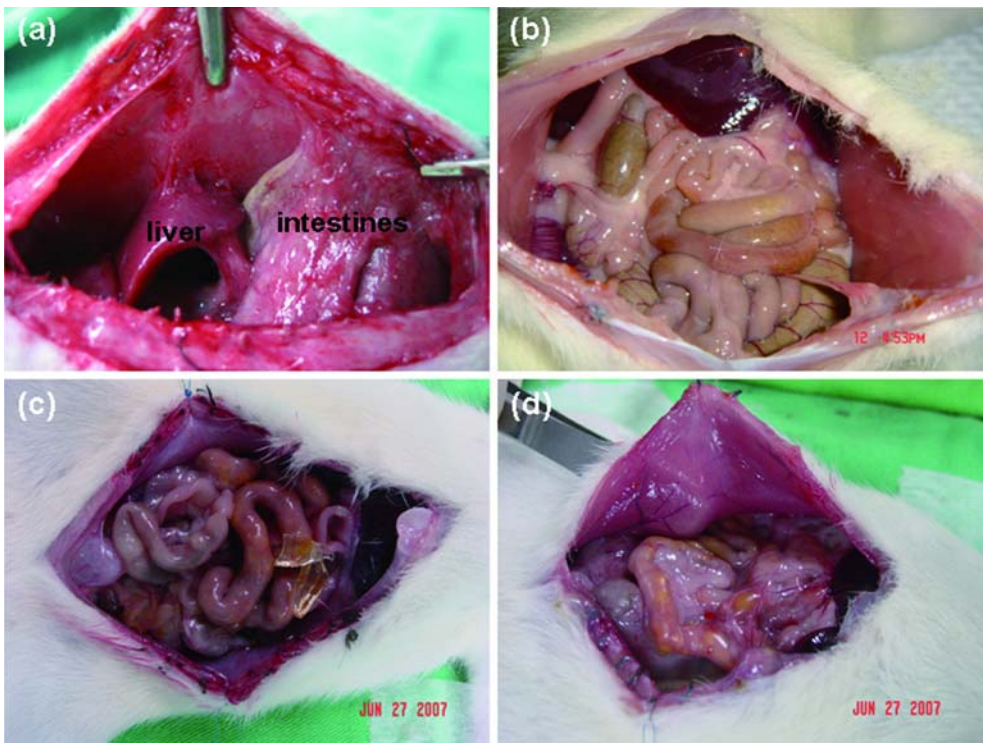

Fig. 7 Repair of the injured sites in the operated rats 28 days after surgery **a** control group **b** treated with P4KL60 film **c** treated with PEML1 film **d** treated with PEML1/G26L35 film

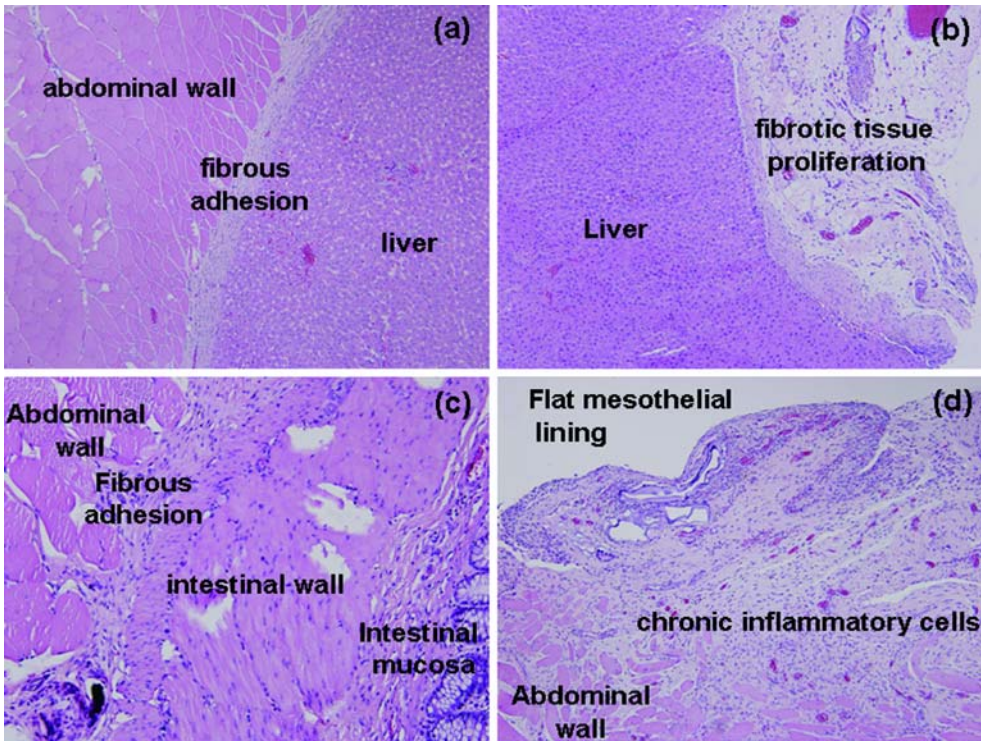

Fig. 8 Histological observation of the wound site on liver surface in rats 28 days after surgery, **a** control group (100×), **b** treated with PEML1 film (100×), the wound site on intestine **c** control group (200×), **d** treated with PEML1 film (100×)

smaller than those of the PEML1 films. Introducing G26L35 with smaller molecular weight leads to faster degradation of the PEML1/G26L35 film. The PEML1 and PEML1/G26L35 films were very effective in preventing tissue adhesion. It can isolate the injured site from adjacent tissues until the injured site is completely healed. Degradation behaviors of various films observed in the animal study were consistent with those investigated by the in-vivo imaging method.

Histological examination

Figure 8 shows the histological observation of the wound site on liver surface in rats. Skeletal muscle of abdominal wall (left) adhered to liver (right) with fibrous adhesion (central) was found at the wound site on liver surface in rats of the control group (Fig. 8a). For the rats treated with PEML1 film (Fig. 8b), liver over left side with loose fibrotic tissue proliferation over serosal surface on right side was observed (Fig. 8b). The fibrotic tissue revealed the healing of liver surface from abrasion injury. Flat mesothelial lining over the the fibrotic tissue is seen and that showed the reason of anti-adhesive ability of the barriers. Skeletal muscle of abdominal wall (left) adhered to intestinal wall (middle) with fibrous adhesion was found in rats of the control group (Fig. 8c). Intestinal mucosa is seen on the right side. For the rats treated with PEML1 film (Fig. 8d), skeletal muscle of abdominal wall after destruction (inferior) shows fibrosis and chronic inflammatory cells infiltration over the peritoneal surface was observed. Flat mesothelial lining (superior) over the fibrotic tissue of the serosal surface is observed and that again showed the anti-adhesive ability of the barriers.

In summary, comb-like polymers were synthesized to make flexible and compliant films with good anti-adhesion properties and low cytotoxicity. Introducing G26L35 with smaller molecular weight leads to faster degradation of the PEML1/G26L35 film. All the injured sites in the operated rats covered with the PEML1 and PEML1/G26L35 films presented no adhesion. The PEML1 and PEML1/G26L35 films were very effective in preventing post-surgical tissue adhesion. Degradation behaviors of the marked films can be investigated non-invasively in the in-vivo imaging system by tracking the positions of the fluorescent marks on the small fragments. The fluorescent MEH-PPV polymer-biocompatible PEML1 polymer guest-host materials were used to make the marking dot array on the tissue anti-adhesion films. The cured PEML1 polymers not only acted as binders to fix the marks on the film but also made the marks hydrophilic and biocompatible. Fluorescent signal tracking is a useful noninvasive tool to monitor the in-vivo degradation behavior of biodegradable materials.

Acknowledgments The authors would like to thank the financial support from Feng Chia University and the Taichung Veterans General Hospital(TCVGH-FCU 968207) Taichung, Taiwan, Republic of China.

References

1. Li H, Liu Y, Shu XZ, Gray SD, Prestwich GD (2004) Synthesis and Biological Evaluation of a Cross-Linked Hyaluronan-Mitomycin C Hydrogel. Biomacromolecules 5(3):895–902 doi:10.1021/bm034463j
2. Park SN, Jang HJ, Choi YS, Cha JM, Son SY, Han SH, Kim JH, Lee WJ, Suh H (2007) Preparation and characterization of biodegradable anti-adhesive membrane for peritoneal wound healing. J Mater Sci Mater Med 18(3):475–482 doi:10.1007/s10856-007-2007-z
3. Arnold PB, Green CW, Foresman PA, Rodeheaver GT (2000) Evaluation of resorbable barriers for preventing surgical adhesions. Fertil Steril 73(1):157–161 doi:10.1016/S0015-0282(99)00464-1
4. Kobayashi MK, Toguchida J, Oka M (2001) Development of the shields for tendon injury repair using polyvinyl alcohol-hydrogel (PVAH). J Biomed Mater Res Appl Biomater 58(4):344–351 doi:10.1002/jbm.1027
5. Matsuda S, Se N, Iwata H, Ikada Y (2002) Evaluation of the antiadhesion potential of UV cross-linked gelatin films in a rat abdominal model. Biomaterials 23(14):2901–2908 doi:10.1016/S0142-9612(01)00418-5
6. Oh SH, Kim JK, Song KS, Noh SM, Ghil SH, Yuk SH, Lee JH (2005) Prevention of postsurgical tissue adhesion by anti-inflammatory drug-loaded Pluronic mixtures with sol–gel transition behavior. J Biomed Mater Res 72A(3):306–316 doi:10.1002/jbm.a.30239
7. Lee JH, Go AK, Oh SH, Lee KE, Yuk SH (2005) Tissue anti-adhesion potential of ibuprofen-loaded PLLA-PEG diblock copolymer films. Biomaterials 26(6):671–678 doi:10.1016/j.biomaterials.2004.03.009
8. Miller JA, Ferguson RL, Powers DL, Burns JW, Shalaby SW (1997) efficacy of hyaluronic acid/nonsteroidal anti-inflammatory drug systems in preventing postsurgical tendon adhesions. J Biomed Mater Res 38(1):25–33 doi:10.1002/(SICI)1097-4636(199721)38:1<25::AID-JBM4>3.0.CO;2-J
9. Liu LS, Berg RA (2002) Adhesion barriers of carboxymethylcellulose and polyethylene oxide composite gels. J Biomed Mater Res 63(3):326–332 doi:10.1002/jbm.10211
10. DiZerega GS, Cortese S, Rodgers KE, Block KM, Falcone SJ, Juarez TG, Berg R (2007) A modern biomaterial for adhesion prevention. J Biomed Mater Res Part B Appl Biomater 81B(1):239–250 doi:10.1002/jbm.b.30659
11. Yamaoka T, Takahashi Y, Fujisato T, Lee CW, Tsuji T, Ohta T, Murakami A, Kimura Y (2001) Novel adhesion prevention membrane based on a bioresorbable copoly (ester-ester) comprised of poly-llactide and Pluronic: in vitro and in vivo evaluations. J Biomed Mater Res 54(4):470–479 doi:10.1002/1097-4636(20010315)54:4<470::AID-JBM20>3.0.CO;2-X
12. Wan Y, Chen W, Yang J, Bei J, Wang S (2003) Biodegradable poly(l-lactide)-poly (ethylene glycol) multiblock copolymer: synthesis and evaluation of cell affinity. Biomaterials 24(13):2195–2203 doi:10.1016/S0142-9612(03)00107-8
13. Lee JH, Kim KO, Ju YM (1999) Polyethylene oxide additive-entrapped polyvinyl chloride as a new blood bag material. J Biomed Mater Res Appl Biomater 48(3):328–334 doi:10.1002/(SICI)1097-4636(1999)48:3<328::AID-JBM18>3.0.CO;2-L
14. Lee JH, Lee HB, Andrade JD (1995) Blood compatibility of polyethylene oxide surfaces. Prog Polym Sci 20(6):1043–1079 doi:10.1016/0079-6700(95)00011-4
15. Mohammadi-Rovshandeh J, Farnia SMF, Sarbolouki MN (1998) Synthesis and thermal behavior of triblock copolymers from l-lactide and ethylene glycol with long center PEG block. J Appl Polym Sci 68(12):1949–1954 doi:10.1002/(SICI)1097-4628(19980620)68:12<1949::AID-APP8>3.0.CO;2-L
16. Bae YH, Huh KM, Kim Y, Park KH (2000) Biodegradable amphiphilic multiblock copolymers and their implications for biomedical applications. J Control Release 64(1):3–13 doi:10.1016/S0168-3659(99)00126-1
17. Perlitz C, Licha K, Scholle FD, Ebert B, Bahner M, Hauff P, Moesta KT, Schirner M (2005) Comparison of two tricarbocyanine-based dyes for fluorescence optical imaging. J Fluoresc 15(3):443–454 doi:10.1007/s10895-005-2636-x
18. Smith AM, Duan H, Mohs AM, Nie S (2008) Bioconjugated quantum dots for in vivo molecular and cellular imaging. Adv Drug Deliv Rev 60(11):1226–1240 doi:10.1016/j.addr.2008.03.015
19. Chen H, Wang Y, Xu J, Ji J, Zhang J, Hu Y, Gu Y (2008) Non-invasive Near Infrared Fluorescence Imaging of CdHgTe Quantum Dots in Mouse Model. J Fluoresc 18(5):801–811 doi:10.1007/s10895-007-0307-9
20. Chiu CC, Lin KF, Chou HL (2003) Chain composition dependence of luminescence properties for copolymers of 2-methoxy-5-2'-ethyl-hexyloxy-1,4-phenylenevinylene and 2,3-diphenyl-5-octyl-1,4-phenylenevinylene. J Polym Sci Part Polym Chem 41(14):2180–2186 doi:10.1002/pola.10766
21. Serrano B, Baselga J, Bravo J, Mikes F, Sese L, Esteban I, Pierola IF (2000) Chemical imaging of phase-separated polymer blends by fluorescence microscopy. J Fluoresc 10(2):135–139 doi:10.1023/A:1009439024969
22. Lee MW, Hung CL, Cheng JC, Wang YJ (2005) A new anti-adhesion film synthesized from polygalacturonic acid with 1-ethyl-3-(3-dimethylaminopropyl) carbodiimide crosslinker. Biomaterials 26(18):3793–3799 doi:10.1016/j.biomaterials.2004.10.009